Performance Analysis and Energy Optimization of Wake-Up Receiver Schemes for Wireless Low-Power Applications

Seyed Mazloum, Nafiseh; Edfors, Ove

Published in:
IEEE Transactions on Wireless Communications

DOI:
10.1109/TWC.2014.2334658

2014

Performance analysis and energy optimization of wake-up receiver schemes for wireless low-power applications

Nafiseh Seyed Mazloum and Ove Edfors
Department of Electrical and Information Technology, Lund University, Lund, Sweden
Email: {nafiseh.seyed_mazloum, ove.edfors}@eit.lth.se

***Abstract*—The use of duty-cycled ultra-low power wake-up receivers (WRxs) can significantly extend a node life time in low-power sensor network applications. In the WRx design, both low-power operation of the WRx and wake-up beacon (WB) detection performance are of importance. We present a system-level analysis of a duty-cycled WRx design, including analog front-end, digital base-band, WB structure, and the resulting WB detection and false alarm probabilities. We select a low-power WRx design, with about two orders of magnitude lower power consumption than the main receiver. The associated cost is an increase in raw bit-error rate (BER), as compared to the main receiver, at the same received power level. To compensate, we use a WB structure that employs spreading. The WB structure leads us to an architecture for the digital base-band with a high address-space scalability. We calculate closed form expressions for detection and false alarm probabilities. Using these we analyze the impact of design parameters. The analytical framework is exemplified by minimization of WB transmit energy. For this particular optimization, we also show that the obtained results are valid for all transmission schemes with an exponential relationship between signal-to-noise ratio and bit-error rate, *e.g.*, the binary orthogonal schemes with non-coherent detection used in many low-power applications.**

***Index Terms*—Medium access, wake-up receiver, sensor network, energy optimization, low-power.**

I. Introduction

A long life-time network where the nodes can operate over an extended time period is a main requirement in many sensor network applications. With limited source of energy, both due to node sizes and/or difficult battery replacements, it can be very challenging to fulfill demanding life-time requirements. To optimize the network life-time it is crucial to design an ultra low power communication system [1]–[7]. The use of ultra-low power wake-up receivers (WRxs) can significantly reduce the overall power consumption of the system. Previous studies on WRx schemes mainly address scenarios where delay is the main design requirement and therefore the WRxs monitor the channel continuously [8]–[11]. The energy consumption of the WRx due to continuous channel monitoring, however, becomes dominant in scenarios with rare data packets. Thus, to further lower the system power consumption, we combine the ultra-low power WRxs and duty-cycled channel listening [12], [13]. For this class of WRx schemes, periodic wake-up beacons (WBs) are transmitted ahead of data packets for synchronization of the communicating nodes. The WRx is switched on periodically for a certain time interval to observe the channel, listening for the WB. The WB consists of a preamble and an address part. The main receiver is only powered up when the WRx detects a WB with the correct address. We have shown in [12] that by optimizing the sleep time of a duty-cycled WRx we can minimize energy consumption while meeting delay requirements. It is therefore of interests to further pursue this type of WRx schemes.

TABLE I
Comparison of Wake-up Receiver Designs

Parameter	[14]	[15]	[16]	[17]	[18]	[19]
Operating frequency [GHz]	2.4	2	2.4	0.915	2.4	0.4
Modulation	OOK	OOK	PPM	FSK	OOK	OOK
Sensitivity [dBm] @ BER 10^{-3}	-75	-70	-87	-65	-64	-80
Data rate [kbps]	100	200	250	50	100	50
Noise figure [dB]	-	-	-	23	-	-
Power consumption [μW]	56	52	415	126	51	280
Technology [nm]	180	90	65	90	90	90
Supply voltage	1.8	0.5	1.2	0.75	0.5	1.5

Previous studies on low-power WRxs focus mainly on the design of the analogue front-end for always-on WRx schemes, but these front-ends can of course be used in duty-cycled schemes as well. We list the design parameters of some of these published works in Table I. The largest difference between always-on and duty-cycled schemes is in the digital base-band processing performed to detect WBs. In the always on case the processing is continuous while for the duty cycled case it is done in a block wise (periodic) fashion. In this paper we focus on the latter case and the performance expressions are therefore not directly applicable to always-on schemes.

A WRx is designed for low power operation, typically two orders of magnitude lower than the power consumption of a main transceiver, e.g. in the order of $10\mu W$ under realistic assumptions [11]. To meet strict power consumption requirements, early attempts avoided power-hungry components such as mixers and synthesizers and simple modulation schemes were often selected. One early such design is given in [20], where a competitive power consumption of 65 μW is achieved, at the cost of a -50 dBm WRx sensitivity. Later designs [14]–

[19][1] have refined the design concepts to improve sensitivity and, in several cases, different low-power mixing strategies have been introduced [15]–[17]. Today we see power consumption levels at around 50 μW and corresponding sensitivity levels at about -70 dBm, in the 2.4GHz frequency range used in this paper. These sensitivity levels are typically related to raw bit-error rates (BERs) in the order of 10^{-3}, *cf.* Table I. While the improvements are impressive, the sensitivity levels reached are significantly worse than the ones for main receiver designs, where we allow orders of magnitude higher power consumption. This also means that orders of magnitude higher transmit power is needed when waking up a node, as compared to normal data transmission. Using a single transmitter structure, such large variations in transmit power will make the design more complicated and also less power efficient [21]. We therefore aim for a simple and power efficient solution with a single transmitter, using the same transmit power both for data and wake-up. With a low-power WRx front-end, and the corresponding loss in sensitivity, the raw BER will be higher than the 10^{-3} level normally used for receiver benchmarking. We show that, by applying proper WB structures and digital base-band processing, the processing gain can compensate for the high raw BER, even for very aggressive power savings in the WRx analog front-end. The costs to pay are longer WBs and longer wake-up delays, which may cause congestion in situations with high enough data traffic. However, in extreme low-power networks with rare data transmission and low demands on delay, these costs can be quite tolerable.

If our goal is to optimize an entire wake-up scheme, to achieve as low power consumption as possible, we need to look beyond sensitivity levels and in a more elaborate way take into account mechanisms that influence power consumption. A missed WB leads to additional WB transmissions by the source node and a falsely detected WB leads to an unnecessary power-up of the main transceiver by the WRx. Hence, we should focus our attention on the WB detection performance, and its connection to WB transmit power consumption. A few studies [22], [23] address WB detection performance and digital base-band processing, and there are also studies addressing the entire WRx chain, e.g. [24]. However, none of these attempts to make a complete analysis where system parameters can be optimized.

Our approach is to analyze the complete system-level design of a duty-cycled WRx, including the analog front-end and digital base-band architectures, the WB packet structure, and the resulting WB detection and false alarm probabilities. First we express the characteristics of the analog front-end for the resulting BER in terms of signal to noise ratio. We then select a WB packet structure that allows for high flexibility in the size of the address-space and makes the design an attractive candidate both for small networks as well as massive ones. The choice of the WB structure leads us to an architecture for the digital base-band, where we improve the design as compared to [25]. We show that by adjusting the WB packet parameters we can compensate for increased raw BERs from the analog front-end and achieve adequate levels of WB detection performance, at the same received power levels as the main receiver sensitivity. Finally, given the raw BER characteristics of the analog front-end, the WB structure, and the digital base-band architecture, we perform analytical calculations of WB detection and false alarm probabilities. These probabilities are defined per listening interval which, without loss of generality, simplifies calculations and make them independent of the length of the sleep interval. Having this analytical framework, we have the prerequisites for a complete analysis of energy/power consumption of the entire system, along the lines of what is introduced in [12], where the influence of the length of the sleep interval is included in the energy models rather than in the detection and false-alarm probabilities. Performing such a complete energy analysis is however beyond the scope of this paper and, as an example, we perform a simplified analysis where we focus on the energy required to transmit the WBs. Using this simplified energy model we illustrate how to optimize WB design parameters for different address-space sizes.

This paper is organized as follows. In Section II we give a description of the overall operation of the addressed system. We present a design choice for the WRx analog front-end and propose a basic structure for the WB packet in Section III. In Section IV we further detail a structure for the digital base-band of the WRx and then present analytical expressions for the detection performance of the proposed design configuration. In Section V simulations are performed to validate the analytical expressions and to evaluate the performance of the proposed structure. These expressions are further used in Section VI to determine the optimal design parameters of WRx schemes. Conclusions and final remarks are given in Section VII.

II. Duty-cycled Medium Access

When targeting wireless sensor network applications with low traffic intensity, idle channel listening becomes a dominant source of power consumption. One of the solutions to this problem is duty-cycled channel listening, where the receiver only periodically wakes-up. This can be done using the main receiver [1]–[7], which is also used for data communication, but we can reduce power consumption even more if a dedicated low-power WRx is employed. This concept, Duty-Cycled Wake-up receiver based Medium ACcess (DCW-MAC), was outlined and partly analyzed in [12]. As the medium access is the center of the analysis in this study, we describe the DCW-MAC scheme in some more detail below.

A. DCW-MAC

In the DCW-MAC scheme, as shown in Fig. 1(a), a node consists of a transmitter, a high performance main receiver, and a low-power/high-BER WRx. All these components are switched off when they are not in use, and thereby we can save energy at the receiver side. The transmitter is used both for data and WB transmissions. In data-transmission mode it may

[1]The design presented in [16] is intended for a duty-cycled WRx scheme, but this is not explicitly analyzed.

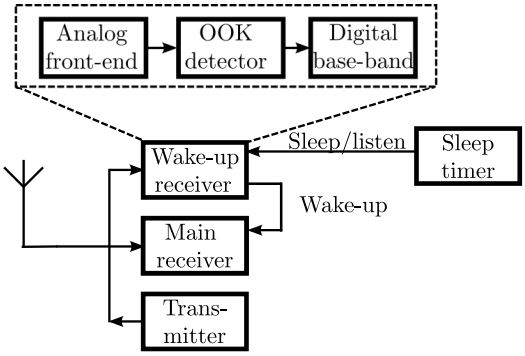

(a) Simplified node architecture block diagram, with control signaling shown. The wake-up receiver is broken down in slightly finer structure.

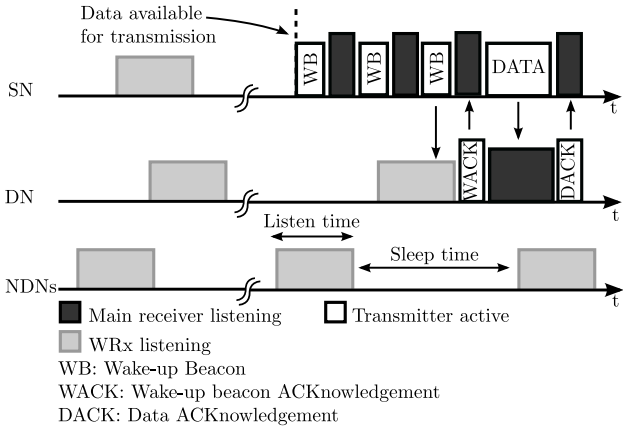

(b) Timing diagram of the DCW-MAC scheme for one packet arrival and a network of N nodes, with one source node (SN), one destination node (DN), and $N-2$ non-destination nodes (NDNs).

Fig. 1. Sensor node architecture and timing diagram used for the DCW-MAC scheme.

use any suitable modulation technique, while in WB transmission mode it resorts to OOK to allow simple low-power detection at the destination node. All nodes in a network share the same radio resource and transmissions are time duplexed. Figure 1(b) shows the timing diagram of the DCW-MAC for one packet arrival and a network of N nodes. The node that has data available for transmission is called the source node (SN), while the intended receiving node is called the destination node (DN). The remaining $N-2$ nodes are what we call non-destination nodes (NDNs), which are the ones that suffer from the false alarms mentioned in the introduction. Periodic WBs are transmitted by the SN ahead of the data packet to synchronize communication between the SN and the DN. The WRxs of all nodes are switched on periodically, in an asynchronous way, and listen to the channel for WBs. The WBs carry both the SN and DN addresses/identities and this way we can avoid overhearing [1] by the NDNs in the network. If the WRx listening interval coincides with a WB transmission with the correct address and the WB is detected, the receiving node switches on its transmitter to reply with a WB acknowledgment (WACK). Between the transmitted WBs the SN is listening to the channel with its main receiver and, when a WACK is received, data transmission is initiated.

One thing that we need to guarantee is that the listening interval of the WRx can cover a complete WB, despite lack of synchronization. In other words, the WRx needs to listen to the channel long enough so that if it barely misses one WB it still has a chance to capture the next one in the same listen interval. This means that the listening interval has to be longer than twice the time-extent of the WB plus the time between the WBs. The time between the WBs is assumed to be long enough to contain a WACK packet. Ideally no error is involved in the detection of the WB, but in reality the transmitted WB is corrupted by noise and possibly interference. This leads to imperfections in terms of detection errors and associated energy costs. While we include the above effects in our analysis, we assume that the data packets are rare and far between, so that effects of collisions can be ignored.

B. Event probabilities and energy costs

As a preparation for the coming analysis of detection errors, let us discuss them in general terms and introduce some of the notation we will use. When we have noise and interference, there is a certain probability that the transmitted WB is missed by the WRx or the WRx accidentally detects a WB that is not there. The latter can happen both when only noise is received or, more likely, when a WB addressed to another node is present on the channel. We will call these events a miss (M) and a false alarm (FA), respectively. The miss event occurs with some probability $P_{\mathrm{M}}^{\mathrm{WB}}$ and generates extra energy consumption in the SN, since additional WBs need to be transmitted before the DN WRx listening time and the SN WB transmission coincide again. The false alarm event happens with a probability $P_{\mathrm{FA}}^{\mathrm{WB}}$ and generates additional energy consumption on the receiver side, since the main transceiver is switched on by the WRx without receiving any data.

The choice of the WB structure as well as the design of the WRx, and the resulting raw BER, highly influence the miss and false alarm probabilities, and consequently the total power consumption of the entire network. For instance, transmission of a long WB may, on the one hand, reduce the miss and false alarm probabilities, and consequently lowers the total energy cost due to WB re-transmissions. A long WB, on the other hand, may also increase the consumed power at both SN and WRx DN. The SN needs to transmit longer WBs and the WRx has to both listen for longer periods and be able to process longer sequences. While this type of mechanisms lead to a complex energy analysis, it also allows us to optimize the total energy consumption in a structured way. Our focus in this paper is on deriving the performance of our wake-up scheme, in terms of $P_{\mathrm{M}}^{\mathrm{WB}}$ and $P_{\mathrm{FA}}^{\mathrm{WB}}$, while we illustrate the principle of energy optimization using a simplified energy model.

To be able to analyze the performance of the wake-up scheme we need to find characterizations of the different parts of the WRx, as shown in Fig. 1(a), and provide a more detailed description of the chosen WB structure.

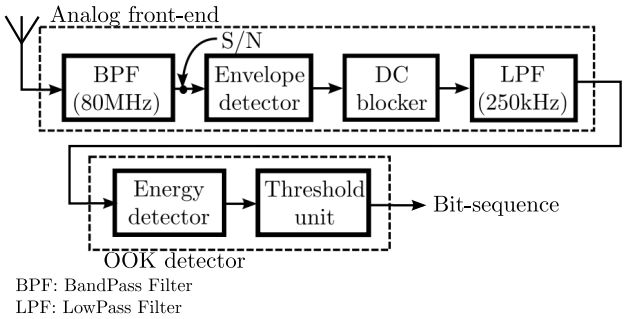

Fig. 2. Simplified block diagram of the low-power/low-complexity WRx analog front-end (AFE) and On-Off Keying (OOK) detector.

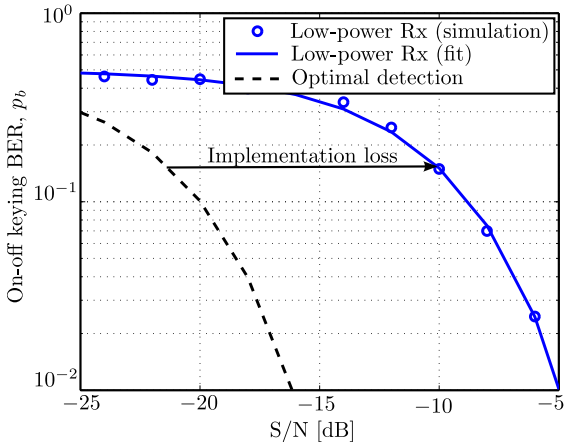

Fig. 3. BER performance of the WRx analog front-end and OOK detector shown in Fig. 2, for an Additive White Gaussian Noise (AWGN) channel. The S/N is measured directly after the 80 MHz wide band-pass filter, at the input of the envelope detector. As reference, we show the BER performance of an optimal OOK detector, operating on the same signal. This shows that our low-power design has about 11 dB implementation loss.

III. Front-end and wake-up beacon structure

As we saw in Table I, different structures are available for design of the analog front-end (AFE) with different characteristics in terms of operating frequency and receiver sensitivity. In these works, different modulation techniques such as OOK, Pulse Position Modulation (PPM), and Frequency Shift Keying (FSK) are used to keep the power consumption of the WRx at a low level. For the analysis in this paper, details like the source of the noise or the choice of the modulation technique is not of prime interest. From a conceptual point of view, as long as the relationship between BER and SNR is known for a certain configuration, the analysis framework of this paper can be applied. Nevertheless, we will use a WRx reference design and characterize its BER vs. S/N performance using simulations.

We have chosen a simple non-coherent OOK modulation for the WB transmission and thereby avoid the use of power-hungry components such as frequency-synthesizer and mixer at the AFE. Figure 2 presents a simplified block diagram of the AFE and OOK detector of the WRx. The RF signal is down-converted to the base-band by an envelope detector. A direct current (DC) blocker and a low-pass filter follow the envelope detector to filter out the DC component and components at the multiples of carrier frequency, generated by the nonlinear characteristics of the envelope detector. The OOK detector measures the energy content of the incoming signal during one symbol interval and converts the base-band signals to a bit-sequence. As mentioned, the drawback of such a design is a generally poor receiver sensitivity. However, our entire WRx design is based on relaxing the requirements on raw BER and thereby allowing it to operate at the same received power level as the main receiver, in our case -90 dBm [13], thus allowing the same transmit power for WB transmission and data. In the following we analyze, by simulation, the performance of the OOK detector and adopt a fitted exponential expression for the BER that later allows us to analytically optimize energy consumption.

A. OOK detector performance simulation

Figure 3 shows the simulated BER performance for an AFE and OOK detector consisting of the above components and in an Additive White Gaussian Noise (AWGN) channel. The design is tailored to the 80MHz wide 2.4GHz ISM band [13] and, to allow for on-chip integration and ultra-low power consumption, the bandwidth of the first filter (bandpass filter) is chosen as the full 80MHz. We further model the envelope detector by a component that outputs the squared input signal. The bandwidth of the low-pass filter is 250kHz to fit the 250kbps data rate [13]. With the binary transmission, the number of information bits per symbol is one where each bit is sampled once. After simulation we find an analytical expression for the raw BER p_b, by curve fitting,

$$p_b = 0.5\,\mathrm{e}^{-12\,\mathrm{S/N}}, \tag{1}$$

where S/N is the SNR at the input of the envelope detector. At this point it is worth noting that the BER resulting from our AFE and OOK detector follows that of other non-coherent detection schemes in that it is an exponential function of the S/N, while the low SNRs are a result of the 80 MHz wide band-pass filter on the input. Comparing to an optimal OOK detector, operating on the same signal, the implementation loss is about 11 dB. This is the price we pay to reduce the power consumption of the WRx in the range of 20 dB compared to the main receiver [11]. Further, the exponential relationship between BER and S/N in (1) will carry through to our energy analysis and optimization in Section VI, making the results more general and valid for all non-coherent detection schemes with the same type of BER relationship.

Since we have deliberately chosen to operate our WRx at the same received power level as the main receiver sensitivity, we will have to operate at very low SNRs on the input. In our numerical examples we use a nominal raw BER of $p_b = 0.15$, operating at $\mathrm{S/N} = -10$ dB. To compensate for these high raw BERs, it is essential to find a WB structure that allows for low-complex/low-power compensation in a digital base-band (DBB) processing.

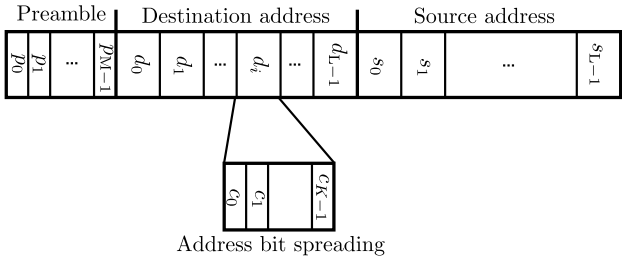

Fig. 4. Wake-up beacon structure consisting of a length M preamble, and length L destination/source addresses. The address bits are, in turn, spread by a K bit sequence.

B. Wake-up beacon structure

A basic WB, as depicted in Fig. 4, should consist of a *preamble*, a *destination address*, and a *source address*. The M-bit preamble sequence, used to detect the presence of a WB and for time synchronization, is selected to be the same for all WBs. The preamble is followed by the L-bit destination and source node addresses. The destination address is needed to prevent power-up of other nodes, while the source address is used in the destination address field of the WACK message.

As we mentioned previously, the WB is received by a high BER front-end and nodes are not synchronized. Therefore, to find an accurate starting-point of the WB and to achieve low probabilities of miss and false alarm, the preamble needs to provide both a processing gain and should be selected from sequences with good auto-correlation properties. We have chosen to generate the preamble using maximum-length shift-register sequences (m-sequences). An important characteristic of an m-sequence is the high peak auto-correlation function while the off-peak values of the auto-correlation function relative to the peak value are small [26]–[28]. For the address bits we do not need good auto-correlation properties, but still need a processing gain to compensate for the high BER. Each bit in both the source and destination address fields is therefore spread by an arbitrary K-bit code[2]. The total number of bits of both source and destination addresses, when spreading is applied, is KL. In this work we select the same spreading, K, for both the destination and source addresses. In principle, however, the spreading can be different.

Additional fields can be attached to the WB to carry information such as maximum number of WBs or the next listen interval of the SN WRx [23], [29]. To keep the analysis tractable, we disregard any such fields and focus on how WRx performance is related to the WB parameters M, K, and L.

IV. Digital base-band

During the listen interval, the front-end of the WRx delivers its received signal in the form of a bit sequence, with a high raw BER since we operate at lower received power than the sensitivity level. The task of the digital base-band (DBB) is to detect the presence of a WB in this bit sequence. We propose a design, based on the WB structure given above, and develop analytical expressions for the detection performance in terms of the WB detection and false alarm probabilities *per listen interval*.[3] The analytical expressions are later used to analyze the WRx operating characteristic for different design parameters.

Fig. 5. Block diagram of a detector consisting of a matched filter (MF) and a threshold unit.

A. Digital base-band design

We use matched filters (MFs) as the main building blocks in our DBB, a very common approach to detect known deterministic sequences in noise. The overall operation of a detector unit is illustrated in Fig. 5. The incoming signal is correlated with the known sequence and whenever the output of the MF exceeds a certain threshold, the sequence is declared to be present by the threshold device.

Figure 6(a) illustrates the proposed DBB design consisting of two detector units and an address decoder. The detector units contain a preamble matched filter (PMF) of length M and an address-spreading matched filter (AMF) of length K, respectively. This particular DBB structure with binary-input matched filters can be implemented with very high energy efficiency, similar to [25]. Initially the DBB can power up only the PMF and search for the preamble to obtain synchronization, since detecting address bits only makes sense after synchronization is obtained. A WB/preamble may arrive at any random time in the listening interval, which is twice the time-extent of the WB $M + 2\,KL$ plus the time-extent of the WACK message δ. The PMF can catch a complete WB only if the WB arrives at a position $i \in [0 \;\; M + 2\,KL + \delta]$, as shown in Fig. 6(b). Note that, since the WACK is received by the main receiver of the SN, no spreading needs to be applied and therefore the WACK window is short compared to the WB length. To simplify the analysis, we therefore set $\delta = 0$ in the remainder of this paper. With the unknown arrival time i of the WB, the PMF may need to correlate the incoming bit-sequence with all the possible arrival times of the preamble, $i \in [0 \;\; M + 2\,KL]$. The MF stops the correlation whenever the PMF output exceeds the decision threshold and announces that a preamble is detected. After the preamble detection, the AMF and the address decoder are activated and the remainder of the input sequence is fed to the AMF, where the individual address bits are detected by correlating the bit-sequence with the address-spreading. Knowing the position of the preamble, the positions of the address bits in the sequence are also known. Therefore, the AMF correlation only needs to be performed once per address bit. Finally, the detected bits are collected by an address decoder and compared against

[2]Even if the choice of spreading code is less critical for the address bits, some sort of pseudo-random code would be used in a real system to avoid a DC level. In our simulations we use m-sequences.

[3]Here we change from using the probability of miss, $P_{\mathrm{M}}^{\mathrm{WB}}$, to using the probability of detection, $P_{\mathrm{D}}^{\mathrm{WB}} = 1 - P_{\mathrm{M}}^{\mathrm{WB}}$, since it will simplify the coming mathematical expressions.

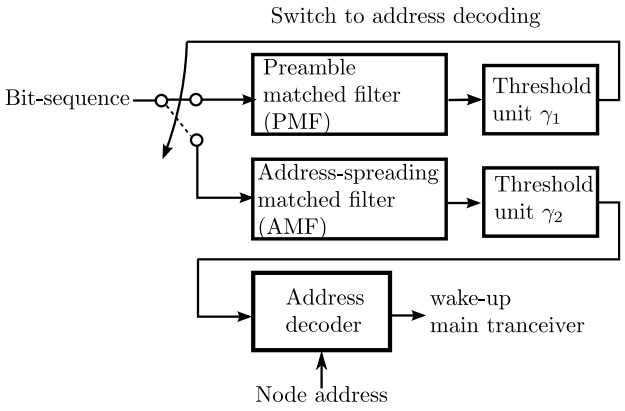

(a) Digital base-band (DBB) block-diagram with a detector for the preamble, a detector for the address bits, and an address decoder.

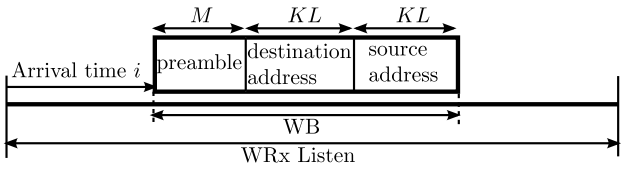

WB length $= M + 2\,KL$
WRx Listen time $= 2\,(M + 2\,KL) + \delta$

(b) Illustration of a wake-up beacon (WB) arriving at time instant i during a WRx listen interval.

Fig. 6. Block diagram of the proposed WRx digital base-band and an illustration of the arrival of a wake-up beacon during a WRx listening interval.

the node address. If the detected address bits match the node address, the main transceiver is powered up.

With the proposed architecture, the PMF and AMF are identical in all nodes in the network. Only the address decoders need to be programmed with the respective node addresses. This leads to a very flexible WRx design, where the node address-space is easily scaled without any major change of the DBB. For instance, to change a network of 256 nodes to a network of 8192 nodes, only the size of the address decoder needs to be increased by 5 bits, while the PMF and AMF can remain unchanged.

B. Detection Performance Analysis

After discussing the overall operation of the DBB, we move on to characterization of the DBB in terms of WB detection and false alarm probabilities. More precisely, the detection probability $P_{\rm D}^{\rm WB}$ is defined as the probability of successful WB detection during one channel listening interval, when a WB is indeed transmitted to the DN. The WB false alarm probability $P_{\rm FA}^{\rm WB}$ is the probability of detecting either a WB with an incorrect address or a non-existing WB, during a WRx listening interval.

The outline of our analysis is as follows. Our DBB consists of two MF-threshold units with slightly different parameters. Therefore, we first express the detection performance of a generic MF-threshold unit and then use these generic expressions to derive closed form expressions for the WB detection and false alarm probabilities.

Let us assume a binary symmetric channel, where the bit errors at the OOK detector occur independently and with probability p_b, for instance given by (1). When the known sequence is present on the channel, the probability $P(n, W)$ that n bits in the sequence of length W are detected correctly, is

$$P(n, W) = \binom{W}{n} (1 - p_b)^n \, p_b^{W-n}. \tag{2}$$

Assuming that the arrival time of the sequence at the MF is known, an MF detects the known sequence correctly with probability

$$\rho^{\rm seq}(\gamma) = \sum_{n=\gamma}^{W} P(n, W) = \sum_{n=\gamma}^{W} \binom{W}{n} (1 - p_b)^n \, p_b^{W-n}, \tag{3}$$

if the number of correct bits n in the length W sequence is above the threshold $\gamma \in [0, W-1]$. When only noise is present on the channel, the OOK detector generates random bits with equal probability. Using (3), the probability that the MF erroneously detects a non-existing sequence therefore becomes

$$\nu^{\rm seq}(\gamma) = (\frac{1}{2})^W \sum_{n=\gamma}^{W} \binom{W}{n}. \tag{4}$$

Now, lets continue with the detection performance of the DBB, using the above generic expressions. A WB is declared to be detected only if both the preamble and the node address are correctly detected. The PMF and AMF outputs used for detection are calculated using different parts of the bit sequence and are therefore independent. Hence, the probability $P_{\rm D}^{\rm WB}$ of detecting a WB when it is present on the channel is equal to the product of the respective detection probabilities of the preamble and the address,

$$P_{\rm D}^{\rm WB} = P_{\rm D}^{\rm pre} P_{\rm D}^{\rm addr}, \tag{5}$$

where $P_{\rm D}^{\rm pre}$ is the probability that the PMF detects the preamble correctly and $P_{\rm D}^{\rm addr}$ is the probability that the address decoder correctly detects the node address. The DBB falsely detects a WB if i) both the preamble and the address code are falsely detected or ii) the preamble is correctly detected, but the address decoder falsely detects an address which belongs to another node. We define the WB interference level, α, as the probability that a WB with an incorrect address is present during the WRx listening. The probability $P_{\rm FA}^{\rm WB}$ that a WB is falsely detected can therefore be calculated as

$$P_{\rm FA}^{\rm WB} = P_{\rm FA}^{\rm pre} P_{\rm FA}^{\rm addr} + \alpha \, P_{\rm D}^{\rm pre} \widetilde{P}_{\rm FA}^{\rm addr}, \tag{6}$$

where $P_{\rm FA}^{\rm pre}$ is the probability that the PMF falsely detects a non-existing preamble, $P_{\rm FA}^{\rm addr}$ is the probability that a non-existing address is erroneously detected as the correct one by the address decoder, and $\widetilde{P}_{\rm FA}^{\rm addr}$ is the probability that the address decoder falsely detects an address, which belongs to another node, as its own.

Below we first detail how to calculate the preamble detection performance $P_{\rm D}^{\rm pre}$ and $P_{\rm FA}^{\rm pre}$ and then turn our attention

to the calculation of the node address detection performance in terms of $P_{\rm D}^{\rm addr}$, $P_{\rm FA}^{\rm addr}$, and $\widetilde{P}_{\rm FA}^{\rm addr}$.

When a WB is present on the channel during the WRx listening interval, the preamble detection probability $P_{\rm D}^{\rm pre}$ is determined by three factors: i) the probability $f(i)$ that the WB arrives at time i, ii) the probability $\rho^{\rm pre}(\gamma_1)$ of detecting the preamble at the correct arrival time i, and iii) the probability $\Omega^{\rm pre}(\gamma_1, i)$ of no erroneous detection of the preamble before time i, where $i \in [0 \quad M + 2\,KL]$ and $\gamma_1 \in [0 \quad M-1]$ is the PMF threshold level. Considering all the possible arrival times of the WB, we get

$$P_{\rm D}^{\rm pre}(\gamma_1) = \sum_{i=1}^{M+2\,KL} \left[f(i)\, \rho^{\rm pre}(\gamma_1)\, \Omega^{\rm pre}(\gamma_1, i) \right]. \qquad (7)$$

Since the nodes are un-synchronized, the arrival time i of the WB is unknown and it is reasonable to assume that all arrival times are equally likely, *i.e.*,

$$f(i) = \frac{1}{M + 2\,K\,L}, \qquad 0 \le i \le M + 2\,KL. \qquad (8)$$

To calculate $\rho^{\rm pre}(\gamma_1)$, we use (3) and substitute the preamble length M and the threshold γ_1 for W and γ. Assuming ideal correlation properties and denoting the probability of a preamble detection at an incorrect time instant by $\nu^{\rm pre}(\gamma_1)$, the probability $\Omega^{\rm pre}(\gamma_1, i)$ becomes

$$\Omega^{\rm pre}(\gamma_1, i) = (1 - \nu^{\rm pre}(\gamma_1))^{i-1}. \qquad (9)$$

To calculate $\nu^{\rm pre}(\gamma_1)$, we assume that detecting a preamble at incorrect timing is equivalent to detecting a preamble when no data is available on the channel, since we assume ideal auto-correlation properties. Using (4), we substitute the preamble length M and the threshold level γ_1 for W and γ. Replacing (8) and (9) back in (7) the preamble detection probability becomes

$$P_{\rm D}^{\rm pre}(\gamma_1) = \frac{1}{M + 2\,K\,L}\, \rho^{\rm pre}(\gamma_1) \sum_{i=1}^{M+2\,KL} (1 - \nu^{\rm pre}(\gamma_1))^{i-1}. \qquad (10)$$

The probability $P_{\rm FA}^{\rm pre}$, that the PMF erroneously detects a preamble when no data is available in the listening interval, is equivalent to the probability that the number of random bits that matches the preamble sequence goes above the threshold γ_1 at least once in the observation interval, *i.e.*,

$$P_{\rm FA}^{\rm pre}(\gamma_1) = 1 - (1 - \nu^{\rm pre}(\gamma_1))^{M+2\,KL-1}. \qquad (11)$$

As shown in (6), to calculate the detection performance of the node address, we consider the operation of the AMF together with the address decoder. The probability $P_{\rm D}^{\rm addr}$ of detecting an address correctly in the address decoder is equal to the probability that the AMF detects all individual address bits correctly. Since the outputs of the AMF are uncorrelated, being based on different parts of the bit sequence,

$$P_{\rm D}^{\rm addr}(\gamma_2) = (\rho^{\rm spcode}(\gamma_2))^L, \qquad (12)$$

where $\rho^{\rm spcode}$ denotes the detection probability of an address bit and is calculated by substituting the spreading code length K and the AMF threshold level $\gamma_2 \in [0 \quad K-1]$ for W and γ in (3).

When there is no data available on the channel, the AMF generates random address bits. Therefore the probability $P_{\rm FA}^{\rm addr}$ that the address decoder falsely announces that the correct address is detected becomes

$$P_{\rm FA}^{\rm addr} = (\frac{1}{2})^L. \qquad (13)$$

Finally, it is likely that a WB which refers to another node is falsely detected. To derive the expression for the probability $\widetilde{P}_{\rm FA}^{\rm addr}$, we introduce q which refers to the number of bits that the nodes own address differs from the address that belongs to another node. Given q, the probability $\widetilde{P}_{\rm FA}^{\rm addr}$ is expressed as

$$\begin{aligned} \widetilde{P}_{\rm FA}^{\rm addr}(\gamma_2) \quad = \quad & \sum_{q=1}^{L} \left[\binom{L}{q} / 2^L \, \left(\rho^{\rm spcode}(\gamma_2)\right)^{L-q} \right. \\ & \left. \left(1 - \rho^{\rm spcode}(\gamma_2)\right)^q \right], \end{aligned} \qquad (14)$$

where $\binom{L}{q}/2^L$ is the probability that q bits are different in randomly chosen L-bit addresses. The second factor is the probability that the AMF detects the $L-q$ matching address bits correctly. The third factor represents the probability that the q non-matching address bits are erroneously detected. We approximate (14) using the fact that errors caused by a single address bit error ($q = 1$) are the most likely,

$$\widetilde{P}_{\rm FA}^{\rm addr}(\gamma_2) \approx \frac{L}{2^L} \, \left(\rho^{\rm spcode}(\gamma_2)\right)^{L-1} \, \left(1 - \rho^{\rm spcode}(\gamma_2)\right). \qquad (15)$$

The analysis below has been performed using both the exact expressions (14) and the approximation (15), without noticeable differences in the results. For the sake of brevity, we only present expressions based on the approximation.

Substituting (7) and (12) in (5) and (11), (13), (7), and (15) in (6) we can calculate the WB detection and false alarm probabilities. The calculation is a relatively straightforward, but tedious, operation that results in

$$\begin{aligned} P_{\rm D}^{\rm WB} \quad = \quad & P_{\rm D}^{\rm pre} P_{\rm D}^{\rm addr} \\ = \quad & \left(\frac{1}{M + 2KL} \rho^{\rm pre}(\gamma_1) \sum_{i=1}^{M+2KL} (1 - \nu^{\rm pre}(\gamma_1))^{i-1} \right) \\ & \left(\rho^{\rm spcode}(\gamma_2)\right)^L \\ = \quad & \left[\frac{1}{M + 2\,KL} \left(\sum_{n=\gamma_1}^{M} \binom{M}{n} (1-p_b)^n \, p_b^{M-n} \right) \right. \\ & \left. \left(\sum_{i=1}^{M+2\,KL} \left(1 - (\frac{1}{2})^M \sum_{n=\gamma_1}^{M} \binom{M}{n} \right)^{i-1} \right) \right] \\ & \left(\sum_{n=\gamma_2}^{K} \binom{K}{n} (1-p_b)^n \, p_b^{K-n} \right)^L, \end{aligned} \qquad (16)$$

and

$$
\begin{aligned}
P_{\mathrm{FA}}^{\mathrm{WB}} &= P_{\mathrm{FA}}^{\mathrm{pre}} P_{\mathrm{FA}}^{\mathrm{addr}} + \alpha P_{\mathrm{D}}^{\mathrm{pre}} \widetilde{P}_{\mathrm{FA}}^{\mathrm{addr}} \\
&= \left(1-(1-\nu^{\mathrm{pre}}(\gamma_1))^{M+2KL-1}\right)(\tfrac{1}{2})^L + \\
&\quad \alpha\left(\frac{1}{M+2KL}\rho^{\mathrm{pre}}(\gamma_1)\sum_{i=1}^{M+2KL}(1-\nu^{\mathrm{pre}}(\gamma_1))^{i-1}\right) \\
&\quad \left(\frac{L}{2^L}\left(\rho^{\mathrm{spcode}}(\gamma_2)\right)^{L-1}\left(1-\rho^{\mathrm{spcode}}(\gamma_2)\right)\right) \\
&= \left[1-\left(1-(\tfrac{1}{2})^M\sum_{n=\gamma_1}^{M}\binom{M}{n}\right)^{M+2KL-1}\right](\tfrac{1}{2})^L + \\
&\quad \alpha\left[\frac{1}{M+2KL}\left(\sum_{n=\gamma_1}^{M}\binom{M}{n}(1-p_b)^n p_b^{M-n}\right)\right. \\
&\quad \left.\sum_{i=1}^{M+2KL}\left(1-\sum_{n=\gamma_1}^{M}\binom{M}{n}(1-p_b)^n p_b^{M-n}\right)^{i-1}\right] \\
&\quad \left[\frac{L}{2^L}\left(\sum_{n=\gamma_2}^{K}\binom{K}{n}(1-p_b)^n p_b^{K-n}\right)^{L-1}\right. \\
&\quad \left.\left(1-\sum_{n=\gamma_2}^{K}\binom{K}{n}(1-p_b)^n p_b^{K-n}\right)\right]. \qquad (17)
\end{aligned}
$$

With the above derivations, we have closed form expressions for the WB detection performance. The rest of the paper will focus on verifying the expressions and illustrating how they can be used to analyze and optimize wake-up receiver schemes.

V. Receiver Operating Characteristics

The analytical expressions for WRx detection performance were derived for ideal correlation properties, while realistic WBs will have a certain amount of auto-correlation. By performing Monte Carlo simulations in MATLAB, using m-sequences both for WB preamble and address spreading we obtain realistic values on WRx performance. By comparing simulated and calculated receiver operating characteristics (ROCs), we both verify the correctness of the analytical derivations and the validity of the ideal-correlation assumptions made. To enhance understanding of the analytical results, we also discuss the overall influence from parameters such as raw BER, preamble length, address spreading length, and network size.

We simulate the behavior of the entire WRx signal chain, detecting WBs, as specified in sections III and IV, for an Additive White Gaussian Noise (AWGN) channel. In the simulation we set the nominal raw BER p_b to 0.15, based on a front-end operating at $\mathrm{S/N} = -10$ dB, *cf.* Fig. 3. The length of the preamble M determines the sharpness of the peak at the PMF output and thereby the preamble detection performance, while the address spreading K determines the performance of the address decoding by the AMF. We change the threshold level $\gamma_1 \in [0, M-1]$ of the PMF, both in the simulations and in the analytical expressions, to evaluate the behavior of the WRx for different choices. As the outputs of the AMF are symmetric, the address bit threshold level is set to the midpoint of the range of possible outcomes, $\gamma_2 = \lceil K/2 \rceil$. Figure 7 shows two example ROCs for a WB with a preamble length $M = 63$, address spreading length $K = 15$, and a network of 256 nodes ($L = 8$). The ROCs are for two levels of WB interference, $\alpha = 1$ and $\alpha = 0.1$. The analytical ROCs match the simulated ones well, but there is a small difference that can be seen in the upper right part of the curve with full WB interference $\alpha = 1$. The analytical expressions over-estimate the false alarm probability somewhat in this region of low to medium threshold levels. The best detection probability $P_{\mathrm{D}}^{\mathrm{WB}}$ of 0.97 is achieved for both cases at a decision threshold γ_1 of 0.76 with a resulting false alarm probability $P_{\mathrm{FA}}^{\mathrm{WB}}$ in the order of $10^{-4} - 10^{-5}$. For lower or higher thresholds γ_1, the most significant effect on the ROC is the reduced detection probability. For low thresholds we find the incorrect preamble position and for high thresholds we miss the preamble entirely. That the false alarm probability stays below a certain value, less than 10^{-2} in this example, for all thresholds is a result of using the destination address to decrease overhearing.

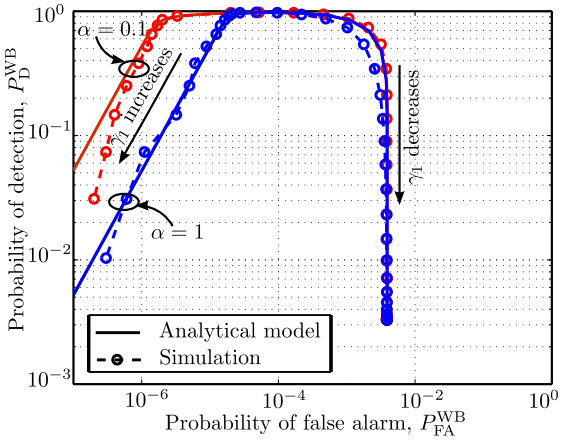

Fig. 7. Simulated and calculated receiver operating characteristics, ROCs, for a wake-up beacon (WB) with a preamble of length $M = 63$, $L = 8$ bit addresses and address spreading $K = 15$, for two different levels of WB interference, $\alpha = 1$ and $\alpha = 0.1$.

In Fig. 7 we can see clear asymptotic behavior of the analytic ROC for small and large threshold levels. By quantifying these, we simplify the interpretation of how different parameters influence the overall WRx detection performance. For high thresholds γ_1, the relationship between $P_{\mathrm{D}}^{\mathrm{WB}}$ and $P_{\mathrm{FA}}^{\mathrm{WB}}$ can be approximated as

$$P_{\mathrm{D}}^{\mathrm{WB}} \approx \frac{1}{\alpha}\frac{\rho^{\mathrm{spcode}}}{L(1-\rho^{\mathrm{spcode}})}\, 2^L\, P_{\mathrm{FA}}^{\mathrm{WB}}. \qquad (18)$$

The rationale behind the approximation is that at high thresholds γ_1, we may miss preambles on the channel, but if they are detected it is most likely in the correct position. Further, at high thresholds, it is also very unlikely that we make a false-alarm if there is no preamble on the channel. Therefore (10) collapses to $P_{\mathrm{D}}^{\mathrm{pre}}(\gamma_1) \approx \rho^{\mathrm{pre}}(\gamma_1)$ and (11) to $P_{\mathrm{FA}}^{\mathrm{pre}}(\gamma_1) \approx 0$, which through (5) and (6) leads to (18). The scaling factor in (18) depends indirectly on the raw BER and the address spreading length, through ρ^{spcode}, while the size of the node

address-space L and the WB interference level α have direct influence.

For low thresholds γ_1, the false alarm probability is, as we mentioned, upper limited by the use of a destination address in the WB. At very low thresholds the probability $P_{\rm FA}^{\rm pre}$ of erroneously detecting a preamble is close to one and the probability of detecting a preamble at its correct position is very low. This essentially leads to entirely random detection of address bits and the probability that the obtained address matches the node address depends only on the size of the address-space – the more address bits, the smaller the probability. In more detail, at low thresholds, (11) collapses to $P_{\rm FA}^{\rm pre}(\gamma_1) \approx 1$ and the WB false alarm probability $P_{\rm FA}^{\rm WB}$ in (6) can be approximated

$$P_{\rm FA}^{\rm WB} \approx (\frac{1}{2})^L. \tag{19}$$

In Fig. 8 we illustrate the principal detection behavior, using the asymptotes (18) and (19), together with corresponding theoretical ROCs. For performance reasons the primary region of interest is where we have high detection probabilities, as indicated in the figure. The nominal design, with full WB interference $\alpha = 1$, is shown as a solid blue line. If, on the one hand, the WB interference level is decreased, $\alpha < 1$, the number of false alarms for high thresholds reduces and the left asymptote is shifted accordingly. As a result, the dotted red ROC curve is obtained and the region of interest increases. If, on the other hand, the detection probability of address bits ρ^{spcode} decreases, we can see in (18) that the false alarm probability for high thresholds increases. As a result, the left asymptote is shifted to the right and the region of interest becomes smaller. Note that a lower ρ^{spcode} is obtained through shorter address spreading K and/or higher raw BER p_b, according to (3) with $W = K$. Reducing the number of bits L in the address-space results in higher number of false alarms for both low thresholds and high thresholds and therefore both asymptotes are shifted accordingly. The region of interest, however, increases as compared to the nominal design. If we reduce the preamble length M the asymptotes stay in place, but the detection probability decreases in the region of interest and the dashed green curve is obtained. The detection probability in the region of interest is also decreased if the raw BER increases[4].

Above we provided a qualitative and quantitative understanding of how different parameters influence the detection performance of the proposed WRx. We have done it by discussing both the full ROC as well as the locations of high- and low-threshold asymptotes.

VI. Optimal Design Parameters

By combining our detailed understanding of how detection performance of the proposed WRx depends on different system parameters with a cost function we can make optimal system designs. Such a cost function will, for sensor networks, typically reflect energy consumption of individual nodes or of the entire network. Assuming that the cost function $J(\boldsymbol{\theta})$ depends on a number of parameters collected in $\boldsymbol{\theta}$ and the permissible range of parameters is $\mathcal{D}$, the optimal system design is given by

$$\boldsymbol{\theta}_{\rm opt} = \underset{\boldsymbol{\theta}\in\mathcal{D}}{\operatorname{argmin}} J(\boldsymbol{\theta}). \tag{20}$$

Most relevant cost functions related to energy will indirectly depend on the ROC of the WRx, as derived above, since detection performance has a fundamental impact on energy consumption. Some of these mechanisms were briefly discussed in Section II.

A comprehensive optimization for an entire network is a very complex task and therefore a topic that needs to be covered separately. Therefore, to illustrate how the ROC expressions can be used for WRx system optimization, we have chosen a simplified case where we are only interested in minimizing the energy used by the source node, SN, to wake up the destination node, DN. When doing this, we also assume that the total energy required at the SN to transmit a WB is proportional to the received WB energy at the DN. The proportionality factor includes transmitter efficiency, propagation losses, etc. These assumptions result in a tractable optimization where we find the optimal WB parameters, preamble length M and address spreading K, for different number of address bits L and raw BERs p_b.

Our cost function can be expressed in terms of the energy required to transmit a single WB, $E_{\rm WB}$, and the average number of WBs, $\bar{\eta}$, needed to activate the DN, according to

$$J(\boldsymbol{\theta}) = E_{\rm WB}(\boldsymbol{\theta})\,\bar{\eta}(\boldsymbol{\theta}), \tag{21}$$

where $\boldsymbol{\theta}$ contains WB parameters we optimize, M and K. In the sequel we will suppress $\boldsymbol{\theta}$ in our expressions.

With the front-end characteristic from (1) the transmitted/received energy per bit is proportional to $-\ln(2\,p_b)$. As we already indicated in Section III, this expression will be the same for all non-coherent schemes where the raw BER is an exponential function of the S/N at the receiver input and the following optimization is therefore valid for all schemes in

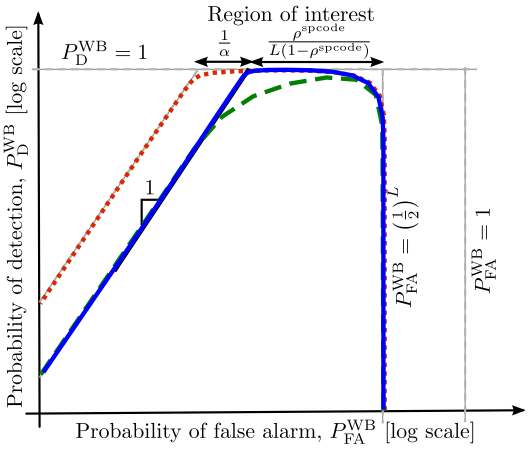

Fig. 8. Illustration of the general properties of the receiver operating characteristic, ROC, for different design parameters, together with the asymptotes in (18) and (19).

[4]Note: A change in BER also affects the location of the left asymptote, as described above.

that class. With this proportionality, the total energy needed to transmit a single WB with a length M preamble and two L bit addresses spread by a factor K is

$$E_{\mathrm{WB}} \propto -\ln(2\,p_b)\,(M + 2\,KL). \tag{22}$$

We will not optimize the sleep time of the WRx, as was done in [12], and simply assume a constant activity factor where the listen period is a constant fraction of the entire sleep-listen cycle. Through this, there will always be a fixed number of WBs per sleep-listen cycle, independent of WB length. Therefore, the average number of WBs transmitted before a successful wake-up, $\bar{\eta}$, is proportional to the average number of sleep-listen cycles, i.e.

$$\begin{aligned}\bar{\eta} &\propto 0.5 + P_{\mathrm{D}}^{\mathrm{WB}} \sum_{k=0}^{\infty} k\,(1 - P_{\mathrm{D}}^{\mathrm{WB}})^k \\ &= \frac{1}{P_{\mathrm{D}}^{\mathrm{WB}}} - 0.5,\end{aligned} \tag{23}$$

which is a result of random starting times, due to asynchronous communication, and a probability $P_{\mathrm{D}}^{\mathrm{WB}}$ of detecting the WB during the listen interval. The proportionality factor is the, in our case fixed, number of WBs per sleep-listen cycle.

Replacing (22) and (23) back in (21), the total energy cost becomes

$$J \propto -\ln(2\,p_b)\,(M + 2\,KL)\,\left(\frac{1}{P_{\mathrm{D}}^{\mathrm{WB}}} - 0.5\right). \tag{24}$$

The optimization parameters M and K influence the total energy through two contradicting mechanisms. Increasing M and K will increase the energy required per transmitted WB, while, at the same time, it decreases the number of WBs required to activate the DN. The balance between these two mechanisms is what our analytical framework provides, in this case, through (16).

Let us move on to numerical optimization of the preamble length M and address spreading K to minimize the energy cost (24) for different raw BERs p_b, for three different sizes of the address-space, namely 4, 8 and 16 address bits. To cover both the reported BERs of the WRx designs in Table I and our choice to use low-power/low-performance front-ends, we perform the optimization for BERs from 0.001 to 0.3. For these parameter ranges, with discrete parameter values, we resort to a quite tractable exhaustive search for 30 values on BER between 0.001 and 0.3. Figure 9 shows the optimal WB length, resulting from the optimal choices of M and K. At low BERs, there is no address spreading ($K = 1$) and only a short preamble is used to obtain synchronization. When the BER increases beyond a certain point, the WB length increases sharply, since additional WB transmissions due to misses are more costly than increasing the WB length. Both preamble length and address spreading are increasing rapidly, but the influence from increases in address spreading changes are more visible, since its influence on the WB length is magnified by the number of address bits.

It is quite natural that increasing BERs lead to longer WBs, in general terms, since detection of them becomes increasingly difficult. However, the relationship between BER and optimal

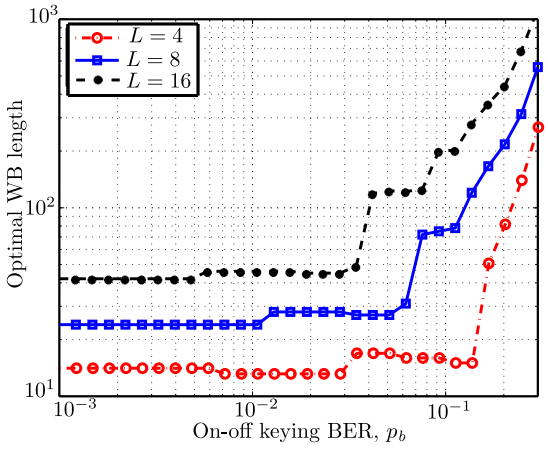

Fig. 9. Optimal wake-up beacon (WB) length vs. OOK raw BER, for address-spaces of size 4, 8 and 16 bits.

WB length is more intricate than that. Perhaps somewhat counter-intuitively, there are also examples of increasing BERs leading to shorter optimal WB-length. Several examples of this can be seen in Fig. 9, especially for the 4-bit address case where the shorter WB lengths make them more visible. In these cases, even if shorter WBs mean lower detection probability and a higher average number of WBs need to be transmitted, the total cost becomes smaller for a shorter WB since it requires less transmission energy.

The cost function we are using in this paper measures the required transmit energy and, as such, it only depends on the detection probability part of the ROC. The detection probabilities resulting from the optimization are shown in Fig. 10(a). The detection probability has a tendency to decrease with increasing BERs, but adjustments of WB length in the optimization brings it back up again when this is favorable from a transmission energy point of view. The largest variations can be seen in the transition regions of BERs where the WB length starts to increase rapidly, as we observed in Fig. 9. The generally shorter WBs for smaller address spaces also lead to the fact that transmission of additional WB due to a miss in the WRx is less costly. Hence, we see that lower detection probabilities can be optimal, from a transmit energy point of view, for smaller address spaces.

False alarm probabilities do not influence our cost function, but the ROC relation implicitly gives us certain false alarm values. These are related to other energy costs in the network, due to unnecessary wake-ups. It is therefore of interest to study these probabilities as well. The false alarm probabilities resulting from the optimization are shown in Fig. 10(b). We can see that they are about 5-10 times lower than the upper asymptote (19) we derived for the ROC (solid line above each curve). For reasonably large address-spaces, the false alarm rates are at very low levels and unnecessary wake-ups should not have a large impact on the total energy consumption of the network. A detailed analysis of these influences is both non-trivial and requires more detailed and complete information about how energy consumption relates to the optimization parameters. While important, this analysis is beyond the scope

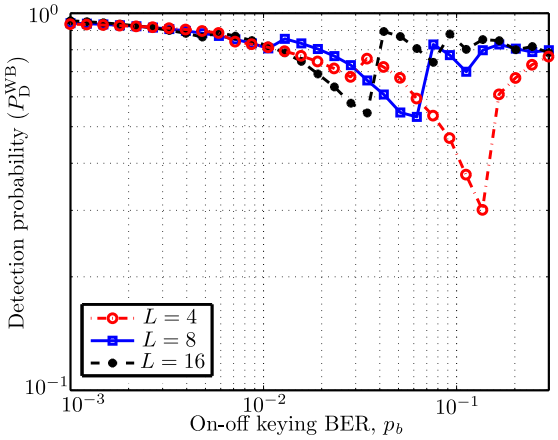

(a) Probability of detection ($P_{\mathrm{D}}^{\mathrm{WB}}$) vs. OOK raw BER.

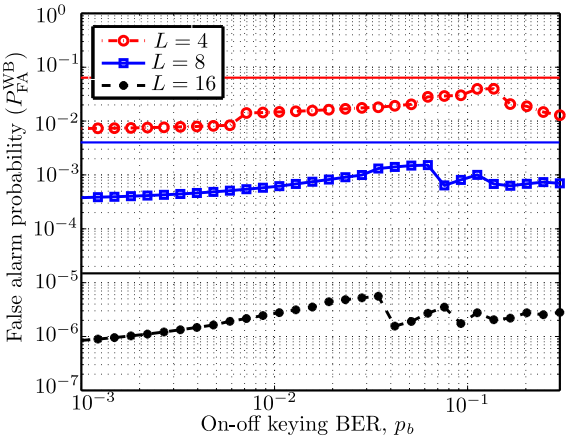

(b) Probability of false alarm ($P_{\mathrm{FA}}^{\mathrm{WB}}$) vs. OOK raw BER. The solid line above each curve is the corresponding upper asymptote (19).

Fig. 10. Optimal probability of detection and the corresponding probability of false alarm, resulting from the optimization, vs. OOK raw BER, for address-spaces of size 4, 8 and 16 bits.

of this paper.

Finally, let us study the optimal transmission energy cost, per wake-up, as a function of raw BER. Since we only know the energy cost up to proportionality, as detailed in (24), we present the normalized optimal WB transmit energies in Fig. 11, for the three investigated address-space sizes. The normalization is with respect to the minimal energy cost for the smallest, 4-bit, address space. For all three address-spaces, we can see that the 10^{-3} BER used as a reference level in previous studies, *cf.* Table I, is not the optimal point of operation when using the duty-cycled wake-up scheme studied in this paper. The optimal BER is closer to 10^{-2} for all three address-spaces and larger address-spaces tend to have a slightly lower optimal BER. When raw BER is lower than the optimal one, the increased transmit power required to lower the BER is larger than the corresponding shortening of the WB, resulting in a higher total energy cost. The differences are, however,

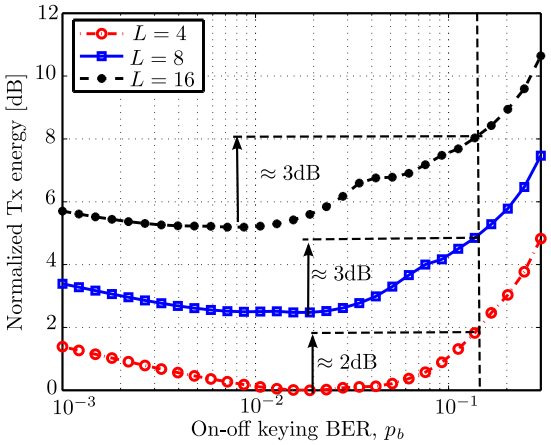

Fig. 11. Optimal wake-up beacon (WB) transmit energies, per wake-up, for different raw BERs and address-spaces of size 4, 8 and 16 bits. Energies are normalized to the minimal energy for the smallest 4-bit address space.

quite small.

Since we aim at using the same transmitter and the same transmit power both for data and wake-up, our low-complexity/low-power WRx will operate at high raw BERs, and in this context the most interesting part of the energy curves is at high BERs. The nominal BER in our WRx design is therefore set to 0.15 , as discussed in Section III, and the additional Tx energy cost as shown in Fig. 11 is only around 2-3 dB. This relatively small additional cost in transmit energy for the SN should be compared to the roughly two orders of magnitude power savings estimated on the WRx side for all nodes in the network.

VII. Conclusions and Remarks

The goal of this paper has been to provide an analysis framework for duty-cycled low-complexity/low-power wake-up receiver schemes, which can be used for design optimization. We perform a complete system-level analysis based on a proposed wake-up beacon structure and the corresponding WRx architecture. The analysis first leads to closed form expressions for detection and false alarm probabilities, as well as qualitative and quantitative understanding of how detection performance relates to changes in design parameters. This understanding of detection performance is fundamental to system-level analysis and optimization of energy consumption. Such an optimization can be done in many different ways, depending on what the ultimate goal is. For instance, it is quite possible to minimize the total power consumption of an entire network, given that we have access to detailed enough information about how energy consumption is related to different design parameters. With limited space we chose to focus on how the detection performance expressions can be used for an optimization of wake-up beacon transmit energy. This means that the presented optimizations are only related to the transmit energy of the source node. While somewhat limited in its scope, the optimization led to several important observations regarding the transmit energy required to successfully activate a destination node. The trade-off between increasing transmit

power and the use of longer beacons becomes evident and a combination of both is required to minimize transmit energy related to WBs at the SN. Based on a specific analog front-end and OOK detection scheme, we also showed that the obtained optimization results are more general and valid for all schemes with an exponential relationship between signal-to-noise ratio and bit-error rate.

In more detail, our analysis shows that it is quite possible to use duty-cycled low-complexity/low-power wake-up receivers, with roughly two orders of magnitude less power consumption in the WRx of all nodes in the network, while allowing the transmitter to use the same transmit power for both wake-up beacons and data. To achieve this, at our chosen nominal raw BER of 0.15, we need to transmit longer beacons than those that give minimal transmit energy. The increase in transmit energy per wake-up is, however, quite moderate at a level of about 2-3 dB for the studied address-space sizes and only applies to the source node.

While analysis and optimization of wake-up beacon transmit energy is performed in detail in this paper, the true value of the analysis framework is that it can be used as a basis for detailed studies and optimization of the energy consumption of entire networks, where other energy models are used. The nature, level of detail, and the particular energy costs taken into account in these depend on the intended application. The analysis framework should also be used to extend the optimization beyond parameters used in this paper. One such example is finding the optimal sleep/listen cycle, along the lines of [12].

Other interesting extensions of the analysis framework is to include more realistic channel models and interference scenarios. As long as we know the relation between SNR and the raw BER on our channel, we can apply the analysis performed in this paper. The only modification needed is to replace (1) with the particular relationship applying to the analyzed channel. While self-interference from the own network is included in the presented analysis, more generic interference types can be included by either adjusting the noise level in the BER expressions or providing a more detailed interference analysis where the properties of the interference signals are more realistic.

REFERENCES

[1] Y. Wei, J. Heidemann, and D. Estrin, "An energy-efficient MAC protocol for wireless sensor networks," in *Proceedings IEEE INFOCOM.*, 2002, pp. 1567–1576 vol.3.

[2] M. Buettner, G. V. Yee, E. Anderson, and R. Han, "X-MAC: a short preamble MAC protocol for duty-cycled wireless sensor networks," in *ACM SenSys.*, 2006, pp. 307–320.

[3] S. Mahlknecht and M. Bock, "CSMA-MPS: A minimum preamble sampling MAC protocol for low power wireless sensor networks," in *Proceedings IEEE International Workshop on Factory Communication Systems.*, 2004, pp. 73–80.

[4] W. Ye, F. Silva, and J. Heidemann, "Ultra-low duty cycle MAC with scheduled channel polling," in *Proc. SenSys*, 2006, pp. 321–334.

[5] A. El-Hoiydi and J.-D. Decotignie, "WiseMAC: An ultra low power MAC protocol for multi-hop wireless sensor networks," in *ISCC.*, 2004.

[6] J. Polastre, J. Hill, and D. Culler, "Versatile low power media access for wireless sensor networks," in *Proc. of the 2nd international conference on Embedded networked sensor systems*, 2004, pp. 95–107.

[7] T. van Dam and K. Langendoen, "An adaptive energy-efficient MAC protocol for wireless sensor networks," in *Proc. of the 1st international conference on Embedded networked sensor systems.*, 2003, pp. 171–180.

[8] M. Lont *et al.*, "Analytical models for the wake-up receiver power budget for wireless sensor networks," in *IEEE GLOBECOM*, 2009, pp. 1146–1151.

[9] C. Guo, L. C. Zhong, and J. Rabaey, "Low power distributed MAC for ad hoc sensor radio networks," in *IEEE GLOBECOM*, vol. 5, 2001, pp. 2944–2948.

[10] Y. Zhang, L. Huang, G. Dolmans, and H. de Groot, "An analytical model for energy efficiency analysis of different wakeup radio schemes," in *IEEE PMIRC*, 2009, pp. 1148–1152.

[11] E.-Y. Lin, J. Rabaey, and A. Wolisz, "Power-efficient rendez-vous schemes for dense wireless sensor networks," in *IEEE International Conference on Communications*, vol. 7, 2004, pp. 3769–3776.

[12] N. S. Mazloum and O. Edfors, "DCW-MAC: An energy efficient medium access scheme using duty-cycled low-power wake-up receivers," in *IEEE VTC Fall*, 2011, pp. 1–5.

[13] H. Sjöland *et al.*, "A receiver architecture for devices in wireless body area networks," *JETCAS*, vol. 2, pp. 82–95, 2012.

[14] X. Yu, J.-S. Lee, C. Shu, and S.-G. Lee, "A 53μW super-regenerative receiver for 2.4 GHz wake-up application," in *IEEE APMC*, 2008, pp. 1–4.

[15] N. M. Pletcher, S. Gambini, and J. Rabaey, "A 52μW wake-up receiver with -72dBm sensitivity using an uncertain-IF architecture," *IEEE J. Solid-State Circuits*, vol. 59, pp. 269–280, 2009.

[16] S. Drago, D. Leenaerts, F. Sebastiano, L. J. Breems, K. A. Makinwa, and B. Nauta, "A 2.4GHz 830pJ/bit duty-cycled wake-up receiver with -82dBm sensitivity for crystal-less wireless sensor nodes," in *IEEE ISSCC*, 2010, pp. 224–225.

[17] M. Lont, D. Milosevic, A. van Roermund, and G. Dolmans, "Ultra-low power FSK wake-up receiver front-end for body area networks," in *RFIC*, 2011, pp. 1–4.

[18] X. Huang, S. Rampu, W. X., G. Dolmans, and H. de Groot, "A 2.4GHz/915MHz 51μW wake-up receiver with offset and noise suppression," in *ISSCC*, 2010, pp. 222–223.

[19] T. Copani, S. Min, S. Shashidharan, S. Chakraborty, M. Stevens, S. Kiaei, and B. Bakkaloglu, "A CMOS low-power transceiver with reconfigurable antenna interface for medical implant applications," *IEEE Transactions on Microwave Theory and Techniques*, vol. 59, pp. 1369–1378, 2011.

[20] N. Pletcher, S. Gambini, and J. Rabaey, "A 65μW, 1.9GHz RF to digital baseband wakeup receiver for wireless sensor nodes," in *IEEE CICC*, 2007.

[21] F. Raab, P. Asbeck, S. Cripps, P. Kenington, Z. Popovic, N. Pothecary, J. Sevic, and N. Sokal, "Power amplifiers and transmitters for RF and microwave," *IEEE Transactions on Microwave Theory and Techniques*, vol. 50, no. 3, pp. 814–826, 2002.

[22] R. de Francisco and Y. Zhang, "An interference robust multi-carrier wake-up radio," in *IEEE WCNC*, 2011, pp. 1265–1270.

[23] Y. Zhang, S. Chen, N. F. Kiyani, G. Dolmans, J. Huisken, B. Busze, P. Harpe, N. van der Meijs, and H. de Groot, "A 3.72μW ultra-low power digital baseband for wake-up radios," in *IEEE VLSI-DAT*, 2011, pp. 1–4.

[24] C. Hambeck, S. Mahlknecht, and T. Herndl, "A 2.4μW wake-up receiver for wireless sensor nodes with -71dbm sensitivity," in *IEEE International Symposium on Circuits and Systems (ISCAS)*, 2011, pp. 534–537.

[25] N. S. Mazloum, J. N. Rodrigues, and O. Edfors, "Sub-Vt design of a wake-up receiver back-end in 65nm CMOS," in *IEEE SubVT*, 2012, pp. 1–3.

[26] J. Borish and J. B. Angell, "An efficient algorithm for measuring the impulse response using pseudorandom noise," *Journal of Audio Engineering Society*, vol. 31, no. 7/8, pp. 478–488, 1983.

[27] M. Cohn and A. Lempel, "On fast m-sequence transforms," *IEEE Transactions on Information Theory*, vol. 23, no. 1, pp. 135–137, Jan 1977.

[28] D. D. Rife and J. Vanderkooy, "Transfer-function measurement with maximum-length sequences," *Journal of Audio Engineering Society*, vol. 37, no. 6, pp. 419–444, 1989.

[29] F. Herrmann, A. Manjeshwar, and J. Hill, "Protocol for reliable, self-organizing, low-power wireless network for security and building automation system," 2003, WO Patent 2,003,061,176.